

## Molecular dynamics computer simulations of solvation in hydrogen bonded systems

Philippe Bopp  
Institut für Physikalische Chemie, Technische Hochschule Darmstadt  
D-6100 DARMSTADT, Federal Republic of Germany

Abstract - This review first discusses briefly some of the various models used in large scale computer simulations of water and aqueous systems. The radial pair distribution functions describing the structures of the hydration shells of divalent ions, as determined from MD simulations of 1.1M solutions of the chloride salts, are then presented. The ion-water potentials for these studies were determined by quantum mechanical ab initio calculations. Then a few typical structural results for non-isotropic systems, such as an aqueous solution near a metal surface or a solvated ion inside a transmembrane channel, are presented. The final sections focus on dynamical results. After a few remarks about correlation functions, the influence of solvated ions on the translational, rotational and vibrational motions of the water molecules are studied. Finally the O-H vibrations in liquid methanol are discussed.

### INTRODUCTION

Computer simulations in general, and molecular dynamics (MD) simulations in particular, have become an increasingly important tool in the study of the liquid state in general. Decisive progress has been achieved with these methods in the study of liquids like water or alcohols with their complex hydrogen bond networks.

In an MD simulations, the atoms of molecules of a chemical system are described as classical point masses or rigid bodies subject to interaction potentials which are assumed to be known. The Newtonian equations of motion for these particles are solved by numerical procedures and the resulting trajectories are then analyzed by computing averages over the ensemble. The computed spacial and time correlations may then be compared with experimental results.

The interaction potentials between the various species present in the chemical system to be studied, the masses, moments of inertia of the particles, and the desired density and total energy are the only input to an MD simulation. From these all macroscopic physical quantities are computed through the simulation, — there are no further adjustable parameters. The results thus depend critically on the potentials employed. The set of interaction potentials which leads to the best agreement between computed and experimental results for as many physical quantities as possible is assumed to be the most realistic description of the system.

### RIGID AND FLEXIBLE MODELS

Simulation studies of molecular liquids have mainly focused on the elucidation of the structure and the intermolecular dynamics (refs. 1). The molecular entities in the liquid have thus mostly been modelled by rigid bodies, neglecting for instance the changes in the molecular geometries due to interactions with neighbouring molecules. The assumption of the molecules as rigid entities is a particularly restrictive one in hydrogen bonded liquids. The hydrogen bond is a comparatively strong and also strongly directed intermolecular interaction; the geometry of a molecule participating in such a bond is known to be different from the gas phase geometry. Marked changes in the frequencies of the vibrational motions between non bonded and bonded molecules (gas and liquid phases) are also usually observed.

Besides not giving access to the phenomena described above, the many models for simulation studies which picture the molecules as rigid bodies neglect the possible consequences of the intramolecular motions and distortions on the structure and dynamics of the liquid. These models are usually called 'rigid' models, among the more prominent ones for water are the ST2 model (ref. 2), the MCY model (ref. 3), the SPC

model (ref. 4), the TIPS (ref. 5) and the TIP4P (ref. 6) models, and many others. In all cases, the interactions are written as combinations of pairwise additive potentials. Results of simulations of water, ice and solutions have been compared with each other in several instances (cf. eg. refs. 1 and 7) and, in spite of the limitations described above, many models have been found to give a very reliable picture of liquid water in many instances.

Stillinger and coworkers (refs. 9) made the first attempt to overcome the limitations of the rigid models in the case of water. They developed a series of models, called the 'flexible central force' models, or briefly CF models, where a single set of three central force potentials ( $V_{OO}$ ,  $V_{OH}$  and  $V_{HH}$ ) was used to describe both the inter- and the intramolecular interaction. In spite of its extreme conceptional simplicity, the last version of this model has been shown to reproduce the structural properties of water and aqueous solutions, as judged from X-ray and neutron scattering functions, quite reliably (refs. 9,10). On the other hand the vibrational motions and the frequency shifts upon condensation were not described adequately (ref. 11).

Subsequently models more realistic in this respect were proposed by Reimers and Watts (RWK2M, ref. 12), Bopp et al. (BJH, ref. 13) and Demontis et al. (DSFG, ref. 14). In the last two cases the intermolecular part of the last version of the CF potential was combined either with an entirely new potential for the intramolecular interactions (ref. 13), or additional potential terms were introduced in this region (ref. 14). In the BJH model, the intramolecular anharmonicities were adjusted in such a way that the correct gas liquid shifts in the three vibrational frequencies of the water molecule are obtained in the classical MD simulations. The BJH model is thus an effective potential.

The approach of combining known and tested intermolecular potentials with new intramolecular ones has subsequently been applied to the MCY model (ref. 15), to the TIPS (ref. 16) and to the SPC models (refs. 16,17). For the MCY model, as well as for the RWK2M model (ref. 12), an additional difficulty arises due to the presence of a force centre (called M) attached to the frame of the rigid molecule, but not located on an atom. If the model is rendered flexible, additional assumptions have to be made concerning the kinematics of this force centre M.

Flexible models have also been developed for non-aqueous hydrogen bonded liquids such as methanol (ref. 18) and other, non-hydrogen bonded liquids like sulphur dioxide (ref. 19), or crown ether (ref. 20). In some of these models, and in most for larger molecules, not all interatomic bonds in a molecule are assumed to be flexible. As the computational expenses rise sharply with the number of interactions to be treated, it is often advisable to keep certain groups (e.g. the  $CH_3$  group in methanol) rigid and to restrict the flexibility to those parts of the molecule where large changes in the bond lengths and in the vibrational motions are to be expected between the gas and the liquid (e.g. the hydrogen bonded O-H in methanol, *vide infra*).

Generally speaking one of the principal advantages of rigid models is the possibility to simulate longer lapses of time at lower computational costs, compared to flexible models. This is due to the fact that in MD simulations the length of an integration increment (time step) is determined by the fastest motion occurring in the system, e.g. a few hundred  $cm^{-1}$  for the hindered rotations of the rigid water molecules and over 3000  $cm^{-1}$  for the oscillations of the flexible molecules. On the other hand a slightly more complex scheme is necessary to integrate the rotational equations of motion. Due to the rigid frame, instantaneous rotations (i.e. librations in a liquid) are well defined quantities. This is not the case with flexible models as in the liquid the notion of 'equilibrium geometry' disappears due to the permanently changing deformation of the molecules. Approximate procedures are thus necessary here to study these motions.

We note here that alternative methods to determine shifts in the vibrational frequencies of molecules have been used besides MD simulations with flexible models. In one instance a perturbational treatment is applied to the gas-phase oscillations with the help of the average forces exerted by the neighbouring molecules on a central molecule as determined from a simulation of the liquid with rigid molecules (ref. 21). Another method is the frozen field local mode approach proposed by Reimers and Watts (refs. 12,27).

Concluding this brief discussion of the principal virtues of flexible and rigid models, it appears that the latter ones are more suited for general studies of systems where the motions have to be followed over long spans of time, while the former ones should be employed for detailed studies of specific problems. Rigid models are still continuously improved with the aim of higher precision and reliability. It was thus possible to include three body intermolecular interactions in an updated version of the MCY model and to study their influence on structural and dynamic properties of pure water (ref. 8), thus lifting another restriction common to all models described above.

## RECENT MD (MOLECULAR DYNAMICS) STUDIES OF AQUEOUS SOLUTIONS

Six interaction potentials are needed to fully describe the interactions in an homogeneous aqueous salt solution: Cation-cation, cation-anion, anion-anion, cation-water, anion-water and water-water. The ion-water and ion-ion potentials may be derived from quantum mechanical 'ab-initio' or semi-empirical calculations, or inferred from experimental quantities like crystal radii and electric multipole moments. They have then to be combined consistently with the water model that has been selected for the simulation. The Coulomb terms of the water-ion potentials are then given by the charges of the ions and by the partial charges assumed for the water molecule in the model, the potentials for the non-Coulomb interactions are usually determined by fitting procedures. A detailed discussion of the various sets of potentials used in MD and MC simulations of aqueous solutions of simple ions and a comparison of the resulting structural properties has been given by Heinzinger (ref. 22).

The studies of 1:1 salt solutions have been continued with studies of a 2.2m *KCl* solution (ref. 25) and a 2.2m *NaClO<sub>4</sub>* solution (ref. 26) with the ST2 model; MC simulations of 0.87m *LiF*, *LiCl*, *KF* and *KCl* solutions with the RKW2M model have been reported (ref. 27). Among others, the studies of isotropic bulk systems have been extended to very high concentrations in the case of *LiCl* (refs. 23). Water and aqueous solutions at high densities, corresponding to pressures of 10 and 20 kbar, have been simulated (refs. 24). The thermodynamics and structure of dense supercritical water has been investigated by Monte Carlo simulations with the rigid TIP52 water model (ref. 45). The availability of simulation of the same, or very similar, systems with different models by different groups have lead to interesting intercomparisons (see e.g. refs. 35). It is through these intercomparisons between different models, as well as through the comparison of simulated and experimental results, that the models can be improved.

A series of 2:1 salt solutions has been simulated (refs. 28-30,34), in one instance also with *D<sub>2</sub>O* as solvent to study the modified dynamical behaviour (ref. 31). A flexible model has been used in these instances to study the intramolecular motions. Furthermore, hydrogen bonded systems in the vicinity of structured solid interfaces have been simulated in several instances (refs. 32,33 and 37). The structure and dynamics of pure water and of a *LiI* solution near a *Pt* [100] crystal surface has been studied both with the ST2 and the BJH models (ref. 32). The dynamics of the hydrated *Na<sup>+</sup>* and *K<sup>+</sup>* ions in a transmembrane channel has been explored (refs. 33). The TIP4P was used in this instance. Such studies require very long simulations and have mostly been conducted with rigid models.

## STRUCTURAL RESULTS FOR THE HYDRATION OF DIVALENT IONS

Several aqueous solutions of 2:1 salts have been studied recently in MD simulations with the flexible BJH water model. The ion water and ion-ion potentials were determined by quantum mechanical ab-initio calculations (cf. ref. 34,46) and fitted to sums of simple pair potentials. Figure 1 shows the ion-oxygen and ion-hydrogen radial distribution functions (RDFs)  $g_{IO}(r_{IO})$  and  $g_{IH}(r_{IH})$  for the divalent cations *Be<sup>++</sup>* (ref. 28), *Mg<sup>++</sup>* (ref. 29), *Ca<sup>++</sup>* (ref. 34) and *Sr<sup>++</sup>* (ref. 30) from MD simulations of 1.1m solutions of the chloride salts of these ions. The hydration numbers, defined as the values *n* of the integral (called the running integration number)

$$n(r) = 4\pi\rho_0 \int_0^r r'^2 g_{IO}(r') dr' \quad (1)$$

up to the ion-oxygen distance  $r_{m1}$  where the corresponding g-function has its first minimum, are reported in Table 1 together with other characteristic data.

At first sight it is obvious that the hydration layers of these ions display a much stronger radial order than the ones of monovalent cations of similar size, see e.g. ref. 22. As expected, and as in the case of the monovalent ions, the height of the first peak in  $g_{IO}(r_{IO})$  decreases with increasing size of the ion (cf. table 1). A pronounced second hydration sphere is present even for the largest cation studied here. On the other hand, in spite of this strong radial order, the lateral order may be much less pronounced than expected. While a hydration number of 6 and an almost perfect octahedral arrangement of the water molecules had previously been found for the hydration shell of the *Mg<sup>++</sup>* ion (refs. 10), a hydration number of slightly more than 9, and thus a hydration shell with very low symmetry, was found for the *Ca<sup>++</sup>* ion. The radial and lateral structure of this hydration sphere was studied in great detail in ref. 37. The hydration number of 9 for the *Ca<sup>++</sup>* ion has also been found in simulations with other model potentials (ref. 38), and has confirmed the neutron inelastic scattering results (ref. 39) obtained with *CaCl<sub>2</sub>* solutions of similar concentrations.

TABLE 1. Characteristic data of the cation-oxygen and cation-hydrogen radial distribution functions from MD simulations of aqueous solutions of 2:1 salts (Distances in Å). The indices  $Mi$ ,  $mi$  and  $i$  refer to the position where the corresponding  $g$ -function has its  $i$ 'th maximum, minimum, and the value 1, respectively.

$\alpha - \beta$	$R_1$	$r_{M1}$	$g_{i\beta}(r_{M1})$	$R_2$	$r_{m1}$	$n$	$r_{M2}$	T [K]
$Be^{++} - O$	1.62	1.75	25.5	2.01	2.3-2.5	6	3.73	310
$Be^{++} - H$	2.23	2.49	7.5	2.76	2.95	12.7	4.59	"
$Mg^{++} - O$	1.88	2.00	19.2	2.24	2.7-2.95	5.8	4.38	320
$Mg^{++} - H$	2.50	2.78	5.2	3.0	3.23	11.63	4.49	"
$Mg^{++} - O(*)$	1.86	2.00	19.2	2.23	2.3-3.0	6.0	4.57	307
$Mg^{++} - H(*)$	2.50	2.75	5.96	2.98	3.2-3.3	12.0	4.90	"
$Ca^{++} - O$	2.23	2.39	14.0	2.72	3.2-3.7	9.2	4.53	300
$Ca^{++} - H$	2.86	3.13	5.98	3.42	3.84	18.7	5.3	"
$Sr^{++} - O$	2.44	2.63	10.6	3.0	3.5-3.7	9.9	5.05	300
$Sr^{++} - H$	3.04	3.38	4.8	3.68	4.00	20.1	5.35	"

\*: simulation with the central force model (refs. 10)

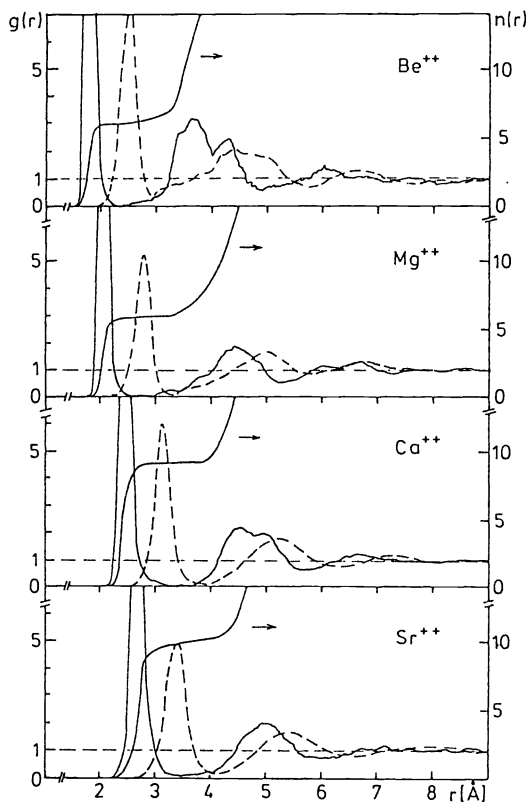


Fig. 1. Radial distribution functions  $g_{IO}(r_{IO})$  and  $g_{IH}(r_{IH})$  and running integration number for the divalent cations from MD simulation of 1.1M chloride solutions.

The water was modelled with the ST2 model, the platinum lattice was treated by means of a nearest neighbour central force model (ref. 40), and the platinum-water potentials were taken as combinations of Lennard-Jones and electrostatic terms (refs. 32,41). The strong order induced by the lattice in the first layer of water molecules above the crystal surface is clearly visible. The interparticle spacing of the platinum atoms on the [100] crystal surface (the crystal surface was not relaxed) is 2.77 Å, very similar to the location of the first peak in the oxygen-oxygen RDF in pure water, ( $R_{M1} = 2.85$  Å). This may in part explain the strong order found in this case. Figure 2 also shows that the surface induced lateral order hardly persists over more than about two layers of liquid above the crystal surface.

The hydration number of 6 found for the  $Be^{++}$  ion is rather unexpected, as most experimental evidence seems to tend towards a value of 4. With such a small ion, which is known to hydrolyze at higher pH, the assumption of pairwise additive potentials may be questioned. On the other hand, rough estimates of the charge transfer and the polarization between this ion and a water molecule (ref. 28) seem to indicate that these effects would not be sufficient to decrease the hydration number from 6 to 4.

In all cases in table 1 the integral over the first peak in  $g_{IH}(r_{IH})$  is equal to, or only very slightly more than twice the value of the corresponding integral over  $g_{IO}(r_{IO})$ . This indicates that, contrary to the monovalent ions, there is virtually no penetration of hydrogen atoms belonging to water molecules of the second hydration layers into the first hydration spheres. The doubly charged central ions are thus able to orient the surrounding water molecules over 2 layers, even at the concentration studied here (cf. ref. 34).

Several MD studies have been conducted to study the very interesting phenomena occurring in the vicinity of solid liquid interfaces, both of electrochemical (ref. 32) and of biological interest (ref. 33). As an example, fig. 2 shows the average local distribution of the water molecules obtained from an MD simulation of pure water near an uncharged platinum [100] surface.

Figure 3 shows the strong order induced by a  $Na^+$  ion in a gramicidine A transmembrane channel filled with water. The TIP4P water model was used here in conjunction with ion-water potentials developed by Bounds (ref. 42), and the interactions with the channel walls were again modelled by Lennard-Jones (12-6) and Coulomb potentials. While the gramicidine skeleton was assumed to be rigid, the  $CO$  groups were flexible and allowed to oscillate. A strong dependence of the water structure in the channel on the number of molecules present was found in this study.

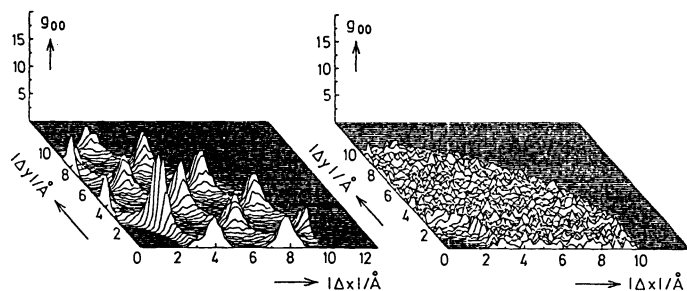


Fig. 2. Distribution  $g_{OO}(|x|, |y|)$  of the water molecules in the first and second water layers adsorbed on an uncharged Pt[100] surface (ref. 32).

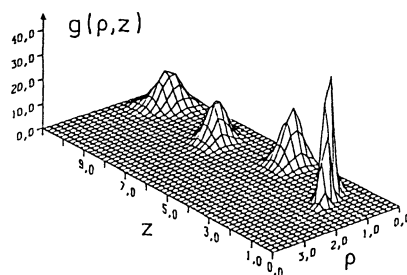


Fig. 3. Distribution  $g_{OO}(\rho, z)$  of the water molecules inside a Gramicidine-A transmembrane channel (ref. 33).

## DYNAMICAL RESULTS

### Time correlation functions

The dynamical behaviour is usually studied by means of correlation functions. Caillol, Levesque and Weis (ref. 43) have recently discussed the basis of the application of the correlation function technique to the determination of static and dynamic dielectric constant in aqueous solutions. Many particle correlation functions have also been reported by Clementi and coworkers (refs. 8 and 15) and used to interpret results of inelastic neutron scattering in pure water. Here we shall restrict ourselves to the study of single particle autocorrelation functions. The autocorrelation function (acf)  $\tilde{c}_{aa}(t)$  of a one particle property,  $a$ , where the quantity  $a$  may for instance be the particle velocity  $\vec{v}_i$  in Cartesian coordinates, is defined as:

$$\tilde{c}_{aa}(t) = \frac{1}{NM} \cdot \sum_i^N \sum_j^M (a_i(t_j) \cdot a_i(t_j + t)) \quad (2)$$

where the  $i$ -sum runs over the  $N$  contributing particles and the  $j$ -sum runs over all time origins  $t_j$ . The normalized autocorrelation function (nacf) is defined accordingly:

$$c_{aa}(t) = \frac{\sum_i^N \sum_j^M (a_i(t_j) \cdot a_i(t_j + t))}{\sum_i^N \sum_j^M (a_i(t_j) \cdot a_i(t_j))} = \frac{\tilde{c}_{aa}(t)}{\tilde{c}_{aa}(0)} \quad (3)$$

The power spectrum  $\hat{c}_{aa}(\omega)$  of the normalized autocorrelation function is defined as:

$$\hat{c}_{aa}(\omega) = \int_0^\infty c_{aa}(t) \cdot \cos(\omega t) dt \quad (4)$$

The acf's of the particle velocities (velocity autocorrelation functions, vacf's) and their power spectra are the mostly used functions to describe the particle motions in the liquid.

The autocorrelation functions may be determined separately for various subensembles in the liquid in order to study for instance the influence of the bonding situation of selected molecules on their motions. The distribution of the molecules into the different subsystems corresponding to the different bonding situations, is usually based on geometric or energetic criteria. It is always performed only at correlation origin ( $t_j$ 's in equations 2 and 3). It is thus assumed that the characteristic times (lifetimes) of the molecules in the subensembles are longer than the characteristic times of the correlations which are examined. This assumption can also be tested to a certain extent by varying the length of the correlation and thus the number of time origins  $t_j$ . The lifetimes of predefined aggregates are also studied by correlation techniques (ref. 44).

In simulations with rigid models, the hindered translations and rotations (librations) of the molecules are studied by computing the autocorrelation functions of the centre of mass velocities and of the angular velocities of the rigid frames (ref. 35). In simulations with flexible models, the  $3N - 6$  vibrational modes of the molecule also appear in the vacf's. The assignment of specific motions in the system to the peaks in the power spectra  $\hat{c}(\omega)$  of the vacf's is possible only in favorable cases, for instance when the peaks are well separated and the frequency shifts are not too large. The bending motion of the water molecule is a case in point. For the other cases, like the stretching motions of the water molecule, or the hindered rotations, vide infra, special correlation functions have to be used to identify and study the individual motions.

The concept of the "equilibrium geometry" of the molecule is central to the usual separation of rotations and vibrations. In the present case, the flexible molecules are always distorted by their interactions with their neighbours in the dense liquid, specially by the hydrogen bonds. These permanent, and also permanently changing, distortions of the molecules do not allow the rigorous definition of an equilibrium configuration which could be used to define a rotating frame and about which the oscillations would be performed. One may rather imagine that the individual molecules perform oscillations of small amplitude about what might be called temporary equilibrium geometries due to their neighbourhoods; these temporary equilibria are in turn expected to change with a time scale similar to the reorientation of the molecule with respect to its neighbours, i.e. much slower than the vibrations themselves.

In the procedure chosen here to analyze the molecular vibrations and librations, the motions actually occurring in the system are used together with the instantaneous molecular geometries to construct correlation functions which approximate the modes of interest. Essentially, the quantities  $a$  (equations 1-3) to be correlated are constructed by combining projections of the instantaneous velocities of the atoms onto bonds or planes of the molecules, as defined by their instantaneous geometries, in a way as to approximate the essential features of a normal coordinate, or of a rotation. The power spectra of the correlation functions of the various  $a$ 's are then constructed and interpreted in the usual way. No assumptions about molecular equilibrium geometries are thus necessary; if one approximation is found to be unsatisfactory for a certain motion, it may easily be replaced by a more sophisticated one. Furthermore, the present technique allows in principle to study cross correlations. However, to reach a sufficient statistical reliability for such cross correlation functions, extremely long MD runs are necessary, we shall thus not discuss them here.

### Translational motions

The translational motions of water and ions in pure water and aqueous ionic solutions have been investigated in several instances (refs. 35 and 47). Furthermore, important studies involving higher correlations (like the current-current autocorrelation function or the intermediate scattering function) have been undertaken recently (refs. 7 and 43).

As an example of the influence of the ions on the motions of the water molecules, fig. 4 shows the power spectra of the acf's of the centre of mass motions of the water molecules in the  $CaCl_2$  solution mentioned above. The functions have been determined separately for three subsystems, namely for water molecules belonging to the first hydration layers of  $Ca^{++}$  and  $Cl^-$ , and for water molecules not belonging to any first hydration layer. We shall term the latter "bulk" water, keeping in mind that, at the concentration of 1.1 molal, they usually belong to a second hydration layer and can thus not be expected to behave dynamically exactly like pure water (cf. ref. 47).

The general shape of the power spectrum  $\hat{c}(\omega)$  for the bulk water is quite similar to the one found for pure water (at a slightly higher temperature) (ref. 48) with the same model, and also quite similar with result found with other models (ref. 7). The prominent feature around  $50cm^{-1}$ , which is usually ascribed to O-O-O bending (ref. 49), is somewhat more pronounced here than for the ST2 model. Compared to pure BJH water, the bulk water spectrum remains virtually unchanged in this region and shows only a small decrease of intensity in the region around  $200cm^{-1}$  ascribed to O-O stretching type motions (ref. 49). A decrease in this region is usually observed with increasing temperature (ref. 2). This indicates that the hydrogen bond network, which is responsible for these motions, is not qualitatively changed by the long range radial order (see  $g_{IO}(r_{IO})$ ) induced by the divalent cation (vide supra). The difference between pure water and bulk water becomes apparent when the diffusion coefficients, which can also be computed from the vacf's, are compared. It has been found (ref. 47), that in a 2.2m  $LiI$  solution about half the difference between the self diffusion coefficient of pure water and of the water in the solution is to be ascribed to the bulk water.

Also surprisingly small, but in excellent agreement with results for  $I^-$  with the ST2 model, are the differences in the spectra of bulk water and the hydration water of  $Cl^-$ . The hydration water shows an increase of intensity in the intermediate region between  $100\text{cm}^{-1}$  and  $200\text{cm}^{-1}$  and a small decrease elsewhere. The water molecules in the first hydration shell of  $Cl^-$  are thus still part of the general H-bond network, the decrease on the high frequency side pointing to an average small loosening of the bonds.

From the spectrum for the hydration water of  $Ca^{++}$  it is obvious that these molecules do no longer participate in this network. The peak at about  $50\text{cm}^{-1}$  has completely disappeared and the entire spectrum is shifted to higher frequencies. This shift is much more pronounced here than in the case of  $Li^+$  studied previously (ref. 47). The shift to higher frequencies reflects the strong binding between ion and water as well as the mutual interactions between the water molecules compressed in the hydration sphere by the strong field of the ion. A band position of  $290\text{cm}^{-1}$  has for instance been reported (ref. 58) from Raman studies for the  $Ca^{++} - H_2O$  stretching vibration.

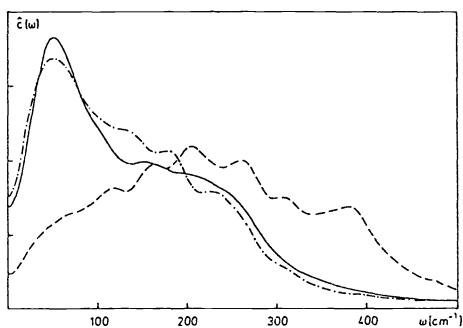


Fig. 4. Power spectra of the centre of mass motions of the water molecules in an aqueous 1.1M  $CaCl_2$  solution. Solid lines: bulk water, dashed lines:  $Ca^{++}$  hydration water, dash-dotted lines:  $Cl^-$  hydration water.

### Librational motions

Figure 5 shows the power spectra obtained by an approximate method (ref. 50) for the three instantaneous rotations of the water molecules, again separately for the three subsystems in the  $CaCl_2$  solution defined above. The axes have been taken in analogy to the three molecule fixed axes in the ST2 model (ref. 47):  $\xi$  perpendicular to the molecular plane,  $\eta$  perpendicular to the dipole moment and in the molecular plane and  $\zeta$  parallel to the molecular dipole moment.

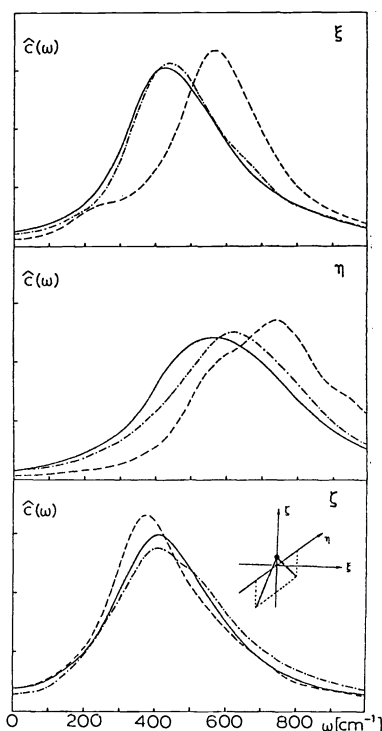


Fig. 5. Power spectra of the librations of the water molecules in an aqueous 1.1M  $CaCl_2$  solution, see fig. 4.

The general features of these spectra are again quite similar to results obtained with the ST2 model. The spectra for the  $\xi$  and  $\zeta$  librations peak at about  $400\text{cm}^{-1}$ , while higher values of approximately  $550\text{cm}^{-1}$  and  $750\text{cm}^{-1}$  are found for the  $\eta$  rotation with the present and the ST2 models, respectively. The higher frequency of this libration is due to the low moment of inertia of the water molecule (ref. 47). Due to the fact that, contrary to the ST2 model, the BJH molecule is distorted (lengthening of the O-H distance and reduction of the H-O-H angle, *vide supra*), the average moment of inertia around the  $\eta$  axis increases and the one around  $\zeta$  decreases, so that the molecule becomes more isotropic. Consequently the three librational spectra are more similar to each other.

The spectra obtained for bulk water and  $Cl^-$  hydration water are again quite similar. A small shift to higher frequencies is found for all three rotations in the hydration water, while a very small shift to lower frequencies has been previously found for the hydration water of  $I^-$ . A shift to higher frequencies for the  $\xi$  and  $\eta$  librations and a small shift to lower frequencies for the  $\zeta$  libration are seen in the  $Ca^{++}$  hydration

water. This is exactly the behaviour that is to be expected from structural arguments (ref. 34). The water molecules are mostly radially oriented in the field of the ion in what is usually called dipolar or  $C_{2v}$  orientation, contrary to what is found in simulations of monovalent ions with the ST2 model, where the tilted, trigonal orientation is preferred. Here the strong bond between the cation and the water molecule is thus only felt by the  $\xi$  and  $\eta$  librations here. This bond is stronger than two H-bonds, the bands are consequently shifted to higher frequencies. Two opposite effects affect the  $\zeta$  libration: Firstly the decreased moment of inertia around this axis, and secondly the strength of the H-bonds between water molecules in the first and second hydration shells. From the lowering of the frequencies, and also from the fact that the band is somewhat narrower, it seems that these bonds are somewhat weaker than usual H-bonds. Similar effects as the ones discussed here are also found for the hydration water of the  $Mg^{++}$  ion (ref. 29).

### Vibrational motions

The vibrational motions were studied by the same procedure as the librations. The quality of the separation can be judged from the shape of the correlation functions and their power spectra. Figure 6 shows the correlation functions and fig. 7 the corresponding power spectra over the entire frequency range of 0 to  $4000\text{cm}^{-1}$  for the "bulk" water of the  $CaCl_2$  solution. The time domain in fig. 6 has been chosen such as to allow, on one hand, the correlation functions to decay and on the other hand to permit for a sufficient number of averages. The Fourier transforms show single lines of finite width, indicating that the modes could indeed be separated satisfactorily. Note that the decay times of the modes are of the order of magnitude of the characteristic times of molecular librations. More detailed studies (ref. 50) show that for instance these decay times are shorter in the hydration water of  $Ca^{++}$  than in the bulk, presumably due to the faster librations in this region (refs. 1, and *vide supra*). Table 2 summarizes the results obtained by this technique and by the usual vacf technique for the hydration water of several ions. The average O-H distances of the water molecules in the hydration layers are also given, in the case of  $Cl^-$  separately for the O-H bonded to the ion and for the O-H bonded to other water molecules.

TABLE 2. Frequencies  $\omega_1$  of the symmetric stretching vibration and  $\omega_3$  of the asymmetric stretching vibration from correlation functions approximating the normal coordinates of water; frequency of the peak maximum of the Fourier transform of the vacf of the hydrogens  $\hat{\omega}$ , in  $\text{cm}^{-1}$ ; and average O-H bond lengths, in Å, for pure water and for water molecules in the hydration layers of various ions from MD simulations with the BJH model.  $\langle R_{OH} \rangle_W$  is the average length of the O-H not bonded to the central  $Cl^-$  ion.

Ion/System	$\omega_1$	$\omega_3$	$\hat{\omega}$	$\langle R_{OH} \rangle$	$\langle R_{OH} \rangle_W$
pure $H_2O$	$3475 \pm 5$	$3580 \pm 5$	$3527 \pm 5$	0.9755	
$LiCl \cdot 4H_2O$ *	$3216 \pm 20$	$3240 \pm 20$	$3210 \pm 20$	0.989	
$Na^+$	$3433 \pm 15$	$3538 \pm 15$	$3472 \pm 10$	0.977	
$Na^{+ **}$	$3437 \pm 15$	$3537 \pm 15$	$3477 \pm 10$	0.978	
$Be^{++}$	$3119 \pm 15$	$3176 \pm 15$	-	0.994	
$Mg^{++}$	$3156 \pm 15$	$3216 \pm 15$	$3190 \pm 15$	0.993	
$Ca^{++}$	$3160 \pm 25$	$3285 \pm 15$	$3208 \pm 10$	0.994	
$Sr^{++}$	$3335 \pm 10$	$3462 \pm 10$	-	-	
$Cl^-^a$	$3377 \pm 15$	$3540 \pm 15$	$3467 \pm 10$	0.980	0.975
$Cl^-^b$	$3375 \pm 15$	$3597 \pm 15$	$3492 \pm 15$	0.980	0.976
$Cl^-^c$	$3393 \pm 15$	$3557 \pm 15$	-	-	-
$Cl^-^d$	$3397 \pm 15$	$3598 \pm 15$	$3482 \pm 10$	0.982	0.978
$Cl^-^e$	$3400 \pm 15$	$3580 \pm 15$	$3495 \pm 10$	0.980	0.975
$Cl^-^f$	$3415 \pm 15$	$3545 \pm 20$	-	-	-

\* cationic and anionic contributions cannot be separated at this concentration.

\*\* at a density corresponding to an external pressure of 10 kbar.

<sup>a</sup> in  $NaCl$ , T = 299K; <sup>b</sup> in  $NaCl$  at 10 kbar, T = 300K; <sup>c</sup> in  $BeCl_2$ , T = 310K;

<sup>d</sup> in  $MgCl_2$ , T = 325K; <sup>e</sup> in  $CaCl_2$ , T = 300K; <sup>f</sup> in  $SrCl_2$ , T = 300K.

While frequency shifts for the hydration water of anions had been expected on the basis of extensive experimental evidence (see ref. 51 and references therein), the frequency shifts reported for the cations, and specially for the divalent ones, were quite unexpected when they were first reported (ref. 52). It is also seen that while the monovalent ions induce only small shifts at medium ion concentration, i.e. where each ion is fully hydrated and where there is only little overlap between hydration spheres, they lead to shifts of magnitudes comparable with the ones induced by divalent cations, (and with the gas-liquid shift,  $\approx 300\text{cm}^{-1}$ ), in very highly concentrated solutions. While such large shifts have not been observed in

aqueous solutions, very large shifts due to monovalent cations have been detected in specially prepared ion-water-base complexes (ref. 53). These shifts were shown to depend both on the strength of the base and on the strength of the ion. For the divalent ions, a dependence of the shifts on the sizes of the central ions is also visible, yet it is much less pronounced than could be expected (ref. 54). Thus the shift found here for the  $Ca^{++}$  hydration water is larger than the experimental one (ref. 54), while the one for  $Mg^{++}$  is in reasonable agreement. Note that the temperature is higher by about 25K in the simulation of the  $MgCl_2$  solution, which may also play a role. Very large red shifts of the O-H vibrations, in agreement with the ones reported here, have been found from *ab initio* calculation of  $Be^{++} - H_2O$  complexes (ref. 46).

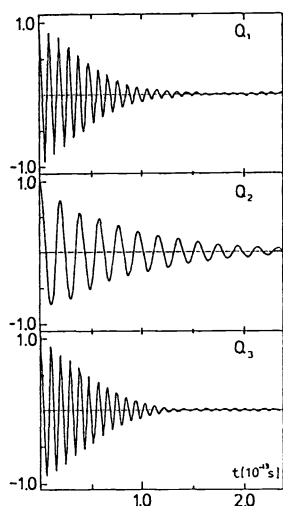


Fig. 6. Correlation functions approximating the three molecular normal modes of a water molecule for the bulk water of a 1.1m  $CaCl_2$  solution.

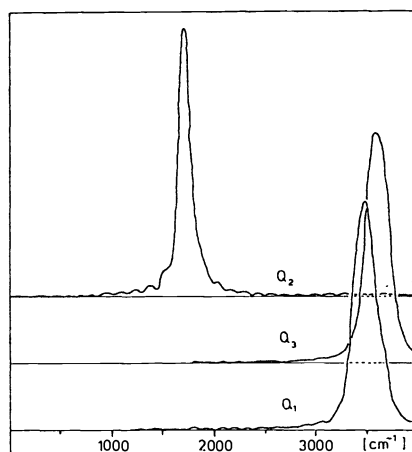


Fig. 7. Power spectra from Fig. 6.

A correlation between the red shift of the vibrational frequencies and the average elongation of the corresponding O-H bonds is found in the simulations, in good agreement with the empirical value of  $\delta\omega/\delta \langle R_{OH} \rangle = -20000cm^{-1}/\text{\AA}$  found experimentally (ref. 55). Elongations of the O-H bond of water molecules in the vicinity of ions have also been determined from NMR measurements (ref. 56) and from *ab initio* calculations (ref. 57) and were found to be in agreement with the ones obtained from the simulations.

The splitting between the asymmetric stretching mode and the symmetric stretching mode  $\Delta\omega = \omega_3 - \omega_1$ , remains at the gas phase value of about  $105cm^{-1}$  in pure liquid water. It stays approximately the same for the hydration water of the cations, except in the case of  $Mg^{++}$  and  $Be^{++}$ , where it is lowered to about  $60cm^{-1}$ . This may be due to the reduction of the H-O-H angle in the hydration water of these ions to values of  $96^\circ$  to  $97^\circ$ , which reduces the kinetic energy coupling, and thus the splitting, between the two O-H oscillators. A reduction of this splitting was also found in the *ab initio* calculations on  $Be^{++} - H_2O$  complexes mentioned above (ref. 46).

Somewhat different values are found for the  $Cl^-$  ion in the various systems studied here. On one hand, the temperatures are not identical in all runs, and on the other hand, the structure of the hydration shell of this ion has been found to depend on the counterion even at low concentrations (0.87, 1.1 and 2.2m) in several instances (refs. 10,27,34). The upper limit of the hydration layer, which is very often not well defined for this ion, is thus not identical for the all the cases. Yet in all cases the splitting  $\Delta\omega$  is markedly increased to 170 to  $190cm^{-1}$ . Comparing the frequencies for the  $Cl^-$  hydration water in table 2 with the ones for pure water it is seen that this increase in  $\Delta\omega$  is due to a much stronger shift of the  $\omega_1$  mode compared to the  $\omega_3$  mode. This is in agreement with results of IR spectroscopy of asymmetric 1:1 water base complexes ( $X^- - HOH$ ) (ref. 59), where the same behaviour has been observed previously. Here it is a consequence of the bonding situation of the water molecules in the hydration layer of  $Cl^-$  with two hydrogen bonds of unequal strength, one directed toward the ion and one toward another water molecule, in good agreement with the structure of the hydration shell as previously determined from the radial distribution functions and angular distribution functions (ref. 34).

The determination of the shifts in the vibrational frequencies is probably one of the most stringent tests of the interaction potentials. A qualitatively correct behaviour of the vibrational modes is found with the

present potentials, which also lead to very satisfactory results for the structure and many other properties. The fact that cations may also induce large shifts was thus suggested by MD simulations. On the other hand, it seems that the potentials may not yet sufficiently reflect the specificity of the various divalent ions in all cases, so that the predictions made by the simulations can be described as being only semiquantitative.

Methanol is another hydrogen bonded system which has been studied by MD simulations with a flexible model. Figure 8 shows the power spectra for the O-H stretching motion from a simulation of liquid methanol with a model similar to the BJH model for water (ref. 18). In this approach the  $CH_3$  group is treated as an unstructured unit. The spectra were again determined for three subsystems: Firstly for molecules engaged in a hydrogen bond with a neighbouring molecule as the hydrogen donor, secondly molecules for which the hydrogen is not in a bond, and thirdly molecules which are neither donor nor acceptor of H-bonds. The H-bond was defined here in terms of geometrical arrangements: Molecules with an O-O distance of less than 3.4 Å and an O-O-H (hydrogen bond) angle of less than 25° were termed "bonded".

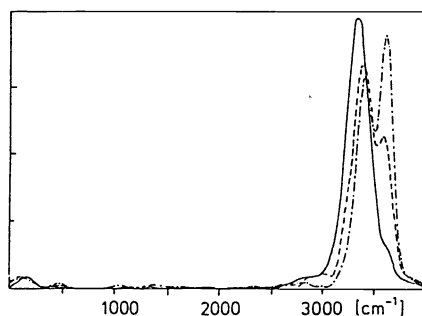


Fig. 8. Power spectra for the O-H oscillations of the  $CH_3OH$  molecule. Solid line: bonded molecules, dashed line: molecules with unbonded O-H group, dash-dotted line: unbonded molecules.

It is seen that the frequency shift correlates rather well with the geometrically determined bonding situation. Bonded molecules (88 % of the cases) show a peak maximum at  $3330 \pm 15 \text{ cm}^{-1}$ , while completely unbonded molecules (3.5 % of the cases) show a peak at  $3610 \text{ cm}^{-1}$  (the gas phase value is  $3690 \text{ cm}^{-1}$ ), and the molecules with unbonded O-H (12 % of the cases) occupy an intermediate position. The origin of the double peaks in the last two cases is not fully understood. This is probably due to the fact that the lifetime of a molecule in the "unbonded subensemble" is of the same order of magnitude as the correlation length. The number of molecules contributing to these functions is also quite small. From this one could tentatively conclude that a frequency shift of about  $80 \text{ cm}^{-1}$  is to be ascribed to the van der Waals type interactions and about  $280 \text{ cm}^{-1}$  to the hydrogen bond.

## SUMMARY AND CONCLUSIONS

Molecular dynamics computer simulations of water, aqueous ionic solutions and of methanol have been used to study the structure as well as the inter and intramolecular dynamics in these liquids. The deformation of the individual molecules by their neighbours, an important effect in the presence of hydrogen bonds, was taken into account. Structural and dynamical results are in good agreement, and satisfactory agreement on a qualitative or semiquantitative level is also found with results obtained from other theoretical methods and from experiments. Further refinements in the model potentials are certainly still required to describe specific phenomena, but in many cases simulations can now be used in a predictive way to study trends in systems not directly accessible experimentally. The analytic and predictive possibility of simulations of hydrogen bonded liquids will be increasingly employed in the future in such fields as biology or geology to study complex systems and interpret experimental results.

## Acknowledgements

It is a pleasure to thank K.Heinzinger, G.Jancsó, G.Pálinkás and E.Spoehr for their interest and for many helpful discussions. J.Brickmann and A.Skerra kindly provided the data for Figure 3 prior to publication.

## REFERENCES

1. K.Heinzinger, Physica **131B**, 196 (1985);  
G.Jancsó, P.Bopp and K.Heinzinger, Acta Chim. Hungarica **121**, 27 (1986).
2. A.Rahman and F.H.Stillinger, J.Chem.Phys. **60**, 1545 (1974).
3. O.Matsuoka, E.Clementi and M.Yoshimine, J.Chem.Phys. **64**, 1351 (1976).
4. H.J.C.Berendsen, J.P.M.Postma, W.F.van Gunsteren, and J.Hermans, in: Intermolecular Forces, edited by B.Pullman, Reidel 1981
5. W.L.Jorgensen, J.Chem.Phys. **77**, 4156 (1982);  
J.Chanderasekhar and W.L.Jorgensen, J.Chem.Phys. **77**, 5080 (1982).
6. W.L.Jorgensen, J.Chanderasekhar, J.D.Madura, R.W.Impey and M.L.Klein, J.Chem.Phys. **79**, 926 (1983).
7. M.D.Morse and S.A.Rice, J.Chem.Phys. **76**, 650 (1982).
8. M.Wojcick and E.Clementi, J.Chem.Phys. **85**, 3544 (1986); *ibid.* **85**, 6085 (1986), and references therein.
9. H.L.Lemberg and F.H.Stillinger, J.Chem.Phys. **62**, 1677 (1975);  
A.Rahman, F.H.Stillinger and H.L.Lemberg, J.Chem.Phys. **65**, 5223 (1975);  
F.H.Stillinger and A.Rahman, J.Chem.Phys. **68**, 666 (1978).
10. P.Bopp, W.Dietz and K.Heinzinger, Z.Naturforsch. **34a**, 1424 (1979);  
W.Dietz, W.O.Riede and K.Heinzinger, Z.Naturforsch. **37a**, 1038 (1982); G.Pálinkás, T.Radnai,  
W.Dietz, Gy.I.Szász, Z.Naturforsch. **37a**, 1049 (1982).
11. P.Bopp and G.Jancsó, Z.Naturforsch. **38a**, 206 (1983).
12. J.Reimers and R.O.Watts, Chem.Phys. **64**, 95 (1981); *ibid.* **85**, 83 (1984); *ibid.* **91**, 201 (1984).
13. P.Bopp, G.Jancsó and K.Heinzinger, Chem.Phys.Letters **98**, 129 (1983).
14. P.Demontis, G.B.Suffritti, E.S.Fois and A.Gamba, J.Mol.Struct. THEOCHEM. **21**, 201 (1985);  
Chem.Phys.Letters **127**, 456 (1986).
15. G.Lie and E.Clementi, Phys.Rev.A **33**, 2679 (1986).
16. L.X.Dang and B.M.Pettitt, in press
17. K.Toukan and A.Rahman, Phys.Rev.B **31**, 2643 (1986);  
R.Bansil, T.Berger, K.Toukan, M.A.Ricci and S.H.Chen, Chem.Phys.Letters **132**, 165 (1986).
18. G.Pálinkás, P.Bopp and K.Heinzinger, in preparation
19. S.Hayashi, M.Oobatake, T.Ooi and K.Machida, Bull.Chem.Soc.Jpn. **58**, 1105 (1985).
20. A.Geiger, in preparation
21. J.P.M.Postma, H.J.C.Berendsen and T.P.Straatsma, J.Phys. **C7**, 45 (1984).
22. K.Heinzinger, Pure & Appl. Chem **57**, 1031 (1985).
23. P.Bopp, I.Okada, H.Ohtaki and K.Heinzinger, Z.Naturforsch. **40a**, 116 (1985);  
K.Tanaka, N.Ogita, Y.Tamura, I.Okada, H.Ohtaki, G.Pálinkás E.Spohr and K.Heinzinger,  
Z.Naturforsch. **42a**, 29 (1987).
24. G.Pálinkás, P.Bopp, G.Jancsó and K.Heinzinger, Z.Naturforsch. **39a**, 179 (1984);  
G.Jancsó, K.Heinzinger and T.Radnai, Chem.Phys.Letters **110**, 196 (1984);  
G.Jancsó, K.Heinzinger and P.Bopp, Z.Naturforsch. **40a**, 1235 (1985);  
G.Jancsó, P.Bopp and K.Heinzinger, Chem.Phys. **85**, 377 (1984).
25. M.Migliore, S.L.Fornili, E.Spohr, G.Pálinkás and K.Heinzinger, Z.Naturforsch. **41a**, 826 (1986).
26. G.Heinje, thesis, Universität Marburg 1986;  
G.Heinje W.A.P.Luck and K.Heinzinger, J.Phys.Chem., **91**, 331 (1987).
27. M.F.Mills, J.R.Reimers and R.O.Watts, Mol.Phys. **57**, 777 (1986).
28. T.Yamaguchi, H.Ohtaki, E.Spohr, G.Pálinkás, K.Heinzinger and M.M.Probst, Z.Naturforsch. **41a**, 1175 (1986).
29. G.Jancsó, P.Bopp and K.Heinzinger, unpublished results.
30. E.Spohr, M.M.Probst and K.Heinzinger, unpublished results.
31. E.Spohr, G.Jancsó, P.Bopp and K.Heinzinger, work in progress.
32. E.Spohr and K.Heinzinger, J.Chem.Phys. **84**, 2304 (1986); Chem.Phys.Letters **123**, 218 (1986);  
E.Spohr, thesis, Johann Gutenberg Universität Mainz 1986
33. W.Fischer, J.Brickmann and P.Läuger, Biophys.Chem. **13**, 105 (1981);  
U.Kappas, W.Fischer, E.E.Polymeropoulos and J.Brickmann, J.Theor.Biol. **112**, 459 (1985);  
A.Skerra and J.Brickmann, Biophys.J., in press
34. M.M.Probst, T.Radnai, K.Heinzinger, P.Bopp and B.M.Rode, J.Phys.Chem. **89**, 753 (1985).
35. G.I.Szász and K.Heinzinger, Z.Naturforsch. **34a**, 840 (1979);  
G.I.Szász, W.O.Riede and K.Heinzinger Z.Naturforsch. **34a**, 1083 (1979);  
G.Pálinkás, T.Radnai, Gy.I.Szász and K.Heinzinger, J.Chem.Phys. **74**, 3522 (1981);  
H.J.Böhm and I.R.McDonald, J.Chem.Soc. Faraday.Trans.2 **80**, 887 (1984);  
W.L.Jorgensen and J.Gao, J.Phys.Chem. **90**, 2174 (1986).

36. R.Kjellander and S.Marcelja, Chemica Scripta **25**, 73 (1985).
37. G.Pálinkás and K.Heinzinger, Chem.Phys.Letters, **126**, 251 (1986).
38. D.G.Bounds, Mol.Phys. **54**, 1335 (1985).
39. N.A.Hewish, G.W.Neilson and J.E.Enderby, Nature(London) **297**, 138 (1982); G.Neilson and J.E.Enderby, Prod.Roy.Soc. A **353**, 390 (1983).
40. J.E.Black and P.Bopp, Surf.Science **140**, 275 (1984).
41. T.Halicioğlu and G.M.Pound, Phys.Stat.Solida **30a**, 619 (1975).
42. D.G.Bounds and P.J.Bounds, Mol.Phys. **50**, 25 (1983).
43. J.M.Caillol, D.Levesque and J.J.Weis, J.Chem.Phys. **85**, 6645 (1986).
44. P.Bopp, in The Physics and Chemistry of Aqueous Ionic Solutions, edited by M-C.Bellissent-Funel and G.W.Neilson, Reidel 1987, in press.
45. A.G.Kalinichev, Int.J.of Thermophysics, **7**, 887 (1986).
46. M.M.Probst, J.R.Limtrakul and B.M.Rode, Chem.Phys.Letters **132**, 370 (1986).
47. Gy.I.Szász, K.Heinzinger and W.O.Riede, Ber.Bunsen.Phys.Chem. **85**, 1056 (1981); Gy.I.Szász and K.Heinzinger, J.Chem.Phys. **79**, 3467 (1983).
48. G.Jancsó, P.Bopp and K.Heinzinger, Chem.Phys. **85**, 377 (1984).
49. M.G.Sceats and S.A.Rice, J.Chem.Phys. **72**, 3236 (1980) and references therein
50. P.Bopp, Phys.Chem. **106**, 205 (1986).
51. W.A.P.Luck, in Structure of Water and Aqueous Solutions, edited by W.A.P.Luck, Physik Verlag und Verlag Chemie, Weinheim 1974
52. M.M.Probst, P.Bopp, K.Heinzinger and B.M.Rode, Chem.Phys. **106**, 317 (1984).
53. H.Kleeberg, G.Heinje and W.A.P.Luck, J.Phys.Chem. **90**, 4427 (1986).
54. O.Kristiansson, A.Eriksson and A.Lindgren, Acta Chem.Scand. **A38**, 609 (1984); O.Kristiansson and A.Eriksson, personal communication.
55. S.J.LaPlaca, W.C.Hamilton, B.Komb and A.Prakash, J.Chem.Phys. **58**, 5206 (1975).
56. J.R.G.van der Maarel, H.R.W.M. de Boer, J.de Bleijser, D.Bedeaux and J.C. Leydte, J.Chem.Phys., in press.
57. M.P.Newton and H.L.Friedmann, J.Chem.Phys. **83**, 5210 (1985).
58. H.Kanno, J.Chem.Phys., in press.
59. D.Schiöberg and W.A.P.Luck, J.Chem.Soc. Faraday Trans. **75**, 762 (1979).